

# Studies on Anisotropic Yield Characteristics and Press Formability of Metal Sheets\* (Investigation into Pure Stretch-Forming)

Yasushi KUROSAKI\*\*, Masanobu MATSUMOTO\*\*\*  
and Masanori KOBAYASHI\*\*\*\*

Based on Bassani yield criterion, a computer simulation of axi-symmetrical pure stretch-forming is attempted. A method for estimating the coefficient of friction necessary for the calculation is presented by extending Hill's method. The results calculated for four kinds of metal sheets are compared with the experimental data. The strain distribution and the fracture position are found to be sensitive to the shape of the yield locus, that is, anisotropic yielding, and it is concluded that the Bassani function is much more useful for the simulation than Hill's old criterion.

**Key Words:** Forming, Pure Stretch-Forming, Computer Simulation, Sheet Metals, Anisotropic Yield Function, Bassani Criterion

## 1. Introduction

Recent development of CAD in sheet metal forming requires an accurate computer simulation for plastic deformation of metal sheets. Studies on the numerical analysis of pure stretch-forming with a rigid punch have been undertaken for the last twenty-five years by many researchers, and the analysis procedures seem to have been established as in the finite difference method (FDM) and the finite element method (FEM). However, there still remains problems to be solved in regard to estimation of the friction coefficient  $\mu$  at the interface between the punch head and the sheet, and a yield criterion (or constitutive equations) to employ as the simulation. In

the present study, a simulation of axi-symmetrical pure stretch-forming with a hemispherical rigid punch is attempted, focusing on these problems.

Kafutanoglu and Alexander<sup>(1)</sup> selected the  $\mu$  values so that the theoretical distribution of the strain components might provide a fit with the experimental data, but their values were anomalously high. This result is reexamined here. Figure 1 shows the radial distribution of the thickness strain  $\epsilon_t$ , obtained by the experiment of pure stretch-forming using commercially pure aluminum sheets and graphite grease lubricant. The  $\mu$  value in this case was estimated as 0.018 by the method mentioned in the next section. The theoretical distribution calculated by the membrane theory employing Hill's quadratic yield criterion (called Hill's old function) is also presented for two stages in Fig. 1. It is seen therefrom that an unusually high value of  $\mu$  is required to make the theoretical curves fit experimental data, which accords with the result by Kaftanoglu and Alexander.

The theory predicts that under a low friction the maximum thinning occurs near the pole ( $s=0$  mm), and thus the fracture also occurs there. However, in the actual forming, the fracture is caused not near the

\* Received 20th May, 1988. Paper No. 87-0340A

\*\* Faculty of Engineering, Mie University, 1515 Kamihama-cho, Tsu, Mie, 514, Japan

\*\*\* Mitsubishi Heavy Industries Co., Ltd., Mihara Factory, 5007 Itosaki-cho, Mihara, Hiroshima, 729-03, Japan

\*\*\*\* Toyota Technical College, 2-1 Eisei-cho, Toyota, Aichi, 471, Japan

pole but at a certain radial position considerably removed therefrom, as exemplified in Fig. 2. This phenomenon had often been experienced, but the reason for it has never been adequately explained by any theories. The present paper will show that these discrepancies between the theory and the experiment are due to an inadequate expression of anisotropy involved in the yield function and can be eliminated by using the Bassani yield function.

2. Estimation of Friction Coefficient

In this section, an estimation method for the friction coefficient  $\mu$  necessary for the numerical analysis of pure stretch-forming is presented. In the metal forming field, various types of friction tests were proposed in the past<sup>(2)</sup>. From the viewpoint of simplicity, a strip compression test by Hill<sup>(3)</sup> is noted here. Although the calibration curves in this test can be determined analytically, it assumes isotropic materials, and thus the trouble with a negative  $\mu$  value arises in the case of materials having planar anisotropy<sup>(4)</sup>. Accordingly, a planar anisotropy was

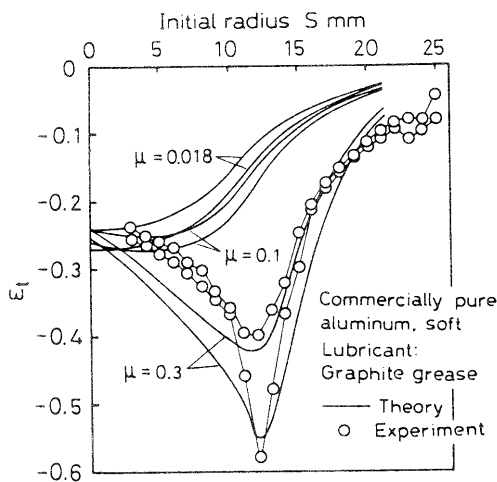
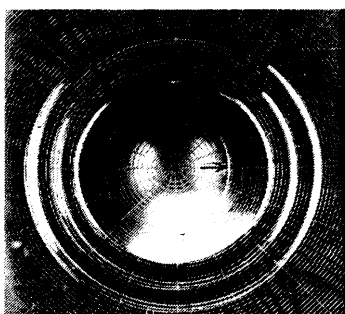


Fig. 1 Comparison of the theoretical and experimental thickness strain distributions based on Hill's old yield function



Material: commercially pure aluminum, soft.  
Lubricant: graphite grease.  
Arrow indicates the fracture position.

Fig. 2 Appearance of a stretch-formed aluminum shell

taken into account for the calibration curves used in the present friction test. For reasons to be mentioned in Chapter 3, the Bassani function<sup>(5)</sup> should be employed here as a yield criterion, but this type of formulation involving planar anisotropy is too complicated. Accordingly, using the Hosford function<sup>(6)</sup>, regarded as better than Hill's old one, the calibration curves were determined by the numerical analysis stated in the following.

2.1 Determination of calibration curves for friction test

A schematic drawing of the calculated model is shown in Fig. 3. Let us consider a narrow and long strip compressed in the thickness direction. The related curve between the nominal longitudinal strain  $(l - l_0)/l_0$  and the nominal thickness strain  $(t_0 - t)/t_0$  is here referred to as a calibration curve, where  $l_0$  and  $l$  are the initial and current lengths, and  $t_0$  and  $t$  are the initial and current thicknesses, respectively. The following are assumed here.

- (1) The strip is sufficiently narrow to neglect  $\sigma_x$ , and the internal shear stress in the strip is also neglected.
- (2) The Coulomb friction rule stands for the interface between the strip and the platens.
- (3) The variation in the strip width does not affect the equilibrium in the longitudinal direction.
- (4) The strip thickness is uniform.
- (5) The principal axes of anisotropy are in accord with the  $x$ -,  $y$ - and  $z$ -axes.

Assumptions (1)~(4) are the same as those employed by Hill. The fundamental equations are as follows.

Equilibrium equation along the  $y$ -axis:

$$d\sigma_y/dy = 2\mu\sigma_z/t \tag{1}$$

Hosford yield function<sup>(6)</sup>:

$$A_1|\sigma_y|^a + A_2|\sigma_z - \sigma_y|^a + A_3|\sigma_z|^a = \sigma_{eq}^a \tag{2}$$

where  $\sigma_y$  and  $\sigma_z$  are principal stresses in the  $y$ - and  $z$ -directions, and  $\sigma_{eq}$  is the equivalent stress. The

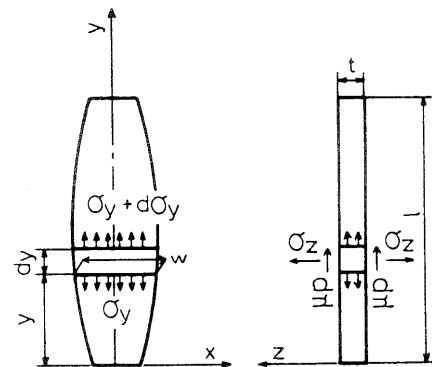


Fig. 3 A calculation model for calibration curves of friction

parameters  $a$ ,  $A_1$ ,  $A_2$  and  $A_3$  are material constants;  $A_1=1/(1+r_y)$ ,  $A_2=1/(1+r_x)$  and  $A_3=1/r_x(1+1/r_y)$ , where  $r_x$  and  $r_y$  are  $r$ -values measured by the tensile test in the  $x$ - and  $y$ - directions, respectively, and  $a=2$ , Eq. (2) reduces to Hill's old function. The other equations used are flow theory relations based on Eq. (1) and a work-hardening equation with  $N$ -th power law. Concerning a boundary condition, an uniaxial compression state  $\sigma_z < 0$  at  $y=0$  was specified. The aforementioned equations were numerically solved for the region  $y > 0$  by the finite difference method. A similar geometry to that recommended by Hill was employed as a strip size, i. e.,  $l_0/t_0=20$  and  $w_0/t_0=2$ , where  $l_0$ ,  $w_0$  and  $t_0$  are the length, width and thickness ( $=0.8$  mm) in the initial state, respectively. The number of the divided elements was taken as 200, and an increment of thickness strain ( $-0.005$ ) was given to every calculation stage. From the numerical solutions obtained for various values of  $\mu$ , the calibration curves for friction were determined.

## 2.2 Friction test condition

Sheets of killed steel, rimmed steel, commercially pure aluminum and OFHC (0.8 mm thick) were employed as test materials. Their respective surface roughnesses were 1.75, 1.83, 0.35 and  $0.47 \mu\text{m}$  in  $Ra$  expression. Their uniaxial properties are shown in Table 1. Test lubricants used were PTFE sheet and graphite grease, graphite grease and three kinds of mineral oils (P01, P3 and St). The surfaces of the specimens were lubricated with these materials before every testing. The specimens were compressed stepwise with a thickness interval of about  $80 \mu\text{m}$  by means of a universal testing machine with 491 kN

maximum capacity. Compression speed was about 0.5 mm/min. The surfaces of the platens (SK3, quenched,  $H_{RC}=60$ ) were lap-finished to produce a roughness  $Ra = 0.07 \mu\text{m}$ .

The size of the specimens was quite small, the same as employed in the aforementioned numerical calculation. Specimens were cut parallel and perpendicular to the rolling direction from the original sheets by means of a micro-saw machine. Hereafter, they are referred to as  $0^\circ$  specimens when their  $y$ -axes are parallel to the rolling direction and as  $90^\circ$  specimens in the perpendicular case, respectively.

It is necessary to determine the Hosford index  $a$  in order to calculate the calibration curves. Hosford<sup>(6)</sup> recommended  $a=8$  for fcc metals and  $a=6$  for bcc metals, but it is not known whether this rule stands in general. Accordingly, the index was experimentally determined through the following procedure. From the Hosford yield function involving triaxial stresses, the stress ratio  $\sigma_p/\sigma_b$  is expressed as

$$\sigma_p/\sigma_b = (r_x + r_y)^{1/a} \{ r_y(1-A)^a + r_x + r_x r_y A^a \}^{1/a} \quad (3)$$

where  $\sigma_p$  and  $\sigma_b$  are yield stresses in the states of plane-strain compression and through-thickness simple compression, respectively, and  $A=1/\{1+r_y^{1/(a-1)}\}$ . From Eq. (3),  $\sigma_p/\sigma_b$  values were calculated for  $a=2, 6$  and  $8$ , and were compared with the experimental data. The experiment was carried out according to the previously reported procedure<sup>(7)</sup>. Thus, a value giving the least difference between the experimental and calculated stress ratios was selected. The result is added to Table 1. The uniaxial tensile test data in the  $y$ -direction was employed as an equivalent stress-

Table 1 Uniaxial properties of metal sheets and various parameters related to yield functions

Materials	Direction	N-value**	r-value*	F MPa**	Tensile strength MPa	Total elongation %	Hosford's index a	Bassani's parameters r m n
Killed steel	0°	0.24	1.74	543	305	37.9	8	1.44 1.20 2.90
	45°	0.22	1.33	549	316	34.5		
	90°	0.23	2.10	531	301	37.6		
	Mean	0.23	1.63	543	310	36.1		
Rimmed steel	0°	0.21	1.09	555	294	36.1	8	1.07 1.20 2.90
	45°	0.20	0.76	566	334	34.3		
	90°	0.21	1.65	553	325	38.1		
	Mean	0.21	1.07	560	322	35.7		
Commercially pure aluminum, soft	0°	0.25	0.70	159	88	30.5	8	0.77 1.10 2.80
	45°	0.26	1.00	154	84	37.2		
	90°	0.28	0.82	161	86	39.5		
	Mean	0.26	0.88	157	86	36.1		
OFHC, soft	0°	0.44	0.90	513	221	44.4	6	0.91 1.10 2.80
	45°	0.44	0.98	501	218	47.6		
	90°	0.45	1.00	509	219	48.3		
	Mean	0.44	0.97	506	219	47.0		

\* : 15 % elongation; \*\*:  $\sigma = F e^N$

equivalent strain relation.

2.3 Result of friction test

An example of the test result is shown in Fig. 4. Similar charts were constructed for various combinations among materials, directions and lubricants, and  $\mu$  values were read out for the nominal thickness strain 0.3. The values for graphite grease to be used in the pure stretch-forming test are presented in Table 2. The differences of  $\mu$  are found to be slight among the materials, but distinct among the directions.

3. Analysis of Pure Stretch-Forming

3.1 Fundamental equations and method for solution

Most of the past works with regard to pure stretch-forming employed the flow rule or generalized constitutive equations based on Hill's old yield function. In the present research, the Bassani yield function<sup>(5)</sup> and the associated flow rule with isotropic hardening, were used. The reasons for it are as follows: anisotropic yielding was regarded as a key point in biaxial tension; this function has a generality

Table 2 Friction coefficients of graphite grease

Materials	0°	90°	Mean
Killed steel	0.022	0.017	0.020
Rimmed steel	0.028	0.013	0.021
Commercially pure aluminum, soft	0.022	0.014	0.018
OFHC, soft	0.019	0.017	0.018

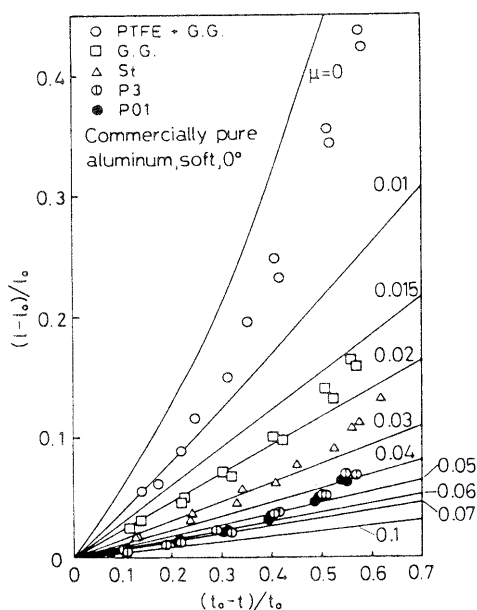


Fig. 4 Examples of friction test results

to express various types of yielding; and no sudden change of stress path is expected to occur before the necking initiation stage. In the previous studies<sup>(7)(8)</sup>, it was shown that the Bassani criterion is useful for predicting yield loci under biaxial tension and the strain distribution in bore-expanding.

A schematic drawing of pure stretch-forming with a rigid hemispherical punch is shown in Fig. 5. Plane stress and planar isotropy were assumed, and a numerical analysis was carried out based on the membrane theory and the finite difference method. The fundamental equations used are as follows.

Bassani yield function<sup>(5)</sup>:

$$S_1^n + \alpha S_2^m = 1 + \alpha \tag{4}$$

where  $S_1 = (\sigma_\phi + \sigma_\theta) / \sigma_{eq}$ ,  $S_2 = (\sigma_\phi - \sigma_\theta) / \sigma_{eq}$ .

Flow rule associated with Eq. (4):

$$\begin{aligned} \frac{d\epsilon_\theta}{S_1^{n-1} - (1+2r)S_2^{m-1}} &= \frac{d\epsilon_\phi}{S_1^{n-1} + (1+2r)S_2^{m-1}} \\ &= \frac{d\epsilon_t}{-2S_1^{n-1}} = \frac{d\epsilon_{eq}}{1 + \alpha + \alpha(m/n-1)S_2^m} \end{aligned} \tag{5}$$

Equilibrium equation:

$$d(t\sigma_\phi) / d\phi = t(\sigma_\theta - \sigma_\phi) \cot \phi + \mu t(\sigma_\theta + \sigma_\phi) \tag{6}$$

Incompressibility condition:

$$dr_\phi / dS = t_0 S \cos \phi / (r_\phi t) \tag{7}$$

Work-hardening rule:

$$\sigma_{eq} = F \left( \int d\epsilon_{eq} \right)^N \tag{8}$$

where  $\sigma_\theta$ ,  $\sigma_\phi$  and  $\sigma_{eq}$  are the circumferential, meridian and equivalent stresses, respectively;  $\alpha = (n/m)(1+2r)$ ;  $m$ ,  $n$  and  $r$  are material constants characterizing anisotropic yielding. Equation (4) can express various yield loci by varying the combination among  $m$ ,  $n$  and  $r$ . The  $d\epsilon_\theta$ ,  $d\epsilon_\phi$ ,  $d\epsilon_t$  and  $d\epsilon_{eq}$  are increments of circumferential, meridian, thickness and equivalent strains, respectively;  $S$  and  $r_\phi$  are the initial and current radial positions, respectively;  $t_0$  and  $t$  are the initial and current thicknesses, respectively, and  $\phi$  is the angle between the normal to the material element and the center axis of the punch. The main procedure for the numerical calculation employed is based on

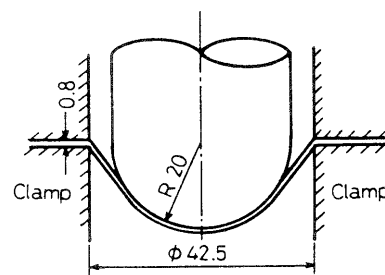


Fig. 5 A calculation model for the numerical analysis of pure stretch-forming

past works<sup>(9)(10)</sup>, except that a program for numerical iteration was needed to determine the stress components from the strain components and their increments. Concerning the boundary conditions, equibiaxial stress and plane-strain ( $d\varepsilon_\theta=0$ ) states were specified at the pole and the clamped edge, respectively. The number of the divided elements was taken as 425, and a thickness strain increment of  $-0.01$  or  $-0.02$  was given to the pole. The computer used is a FACOM M-382, courtesy of the Nagoya University Computer Center.

### 3.2 Pure stretch-forming test

Using the aforementioned four materials, a pure stretch-forming test was carried out by means of a sheet forming machine with a maximum capacity of 98 kN. The tools used were a hemispherical punch, 40 mm in diameter, a die with 42.5 mm aperture diameter, and 5 mm profile radius and a clamping tool<sup>(10)</sup>. The clamping force was 76 kN and the punch speed was 0.2 mm/s. The punch surface was lubricated with the graphite grease before every testing. Square blanks of  $88 \times 88 \text{ mm}^2$  were cut from the original sheets, and radial lines with an angle interval of  $22.5^\circ$  and concentric circles with a diameter interval of 2 mm were scribed on their surfaces by means of a photo-etching technique.

### 3.3 Results and discussion

Calculations were carried out for the aforementioned four metals and graphite grease lubrication. The friction coefficients  $\mu$  were selected from the mean values in Table 2, and  $N$  and  $F$  from the planar mean values in Table 1. The Bassani parameters were quoted from the measurements of the bore-expanding test<sup>(8)</sup> and are shown in Table 1.

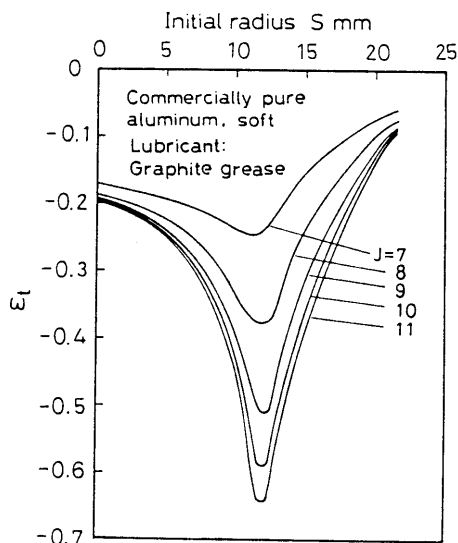


Fig. 6 Theoretical distribution of thickness strain

An example of theoretical results is shown in Fig. 6, giving the radial distribution of the thickness strain  $\varepsilon_t$  for five stages ( $J=7\sim 11$ ) in the case of aluminum sheets. The corresponding experimental result (averages in three directions  $0^\circ$ ,  $45^\circ$  and  $90^\circ$ ) is shown in Fig. 7. From Figs. 6 and 7, it can be concluded that the present calculation well predicts the experimental result, and thus does not require such an unreasonable adjustment with  $\mu$  values as mentioned in Chapter 1. The distributions of  $\varepsilon_t$  and  $\varepsilon_\theta$  are compared between the theory and the experiment in Figs. 8 (a) and (b), where the theoretical curves based on Hill's old function ( $m=n=2$ ) are also given. Although the present simulation is not perfect, it is markedly improved especially in the  $\varepsilon_t$  distribution by changing Hill's old function for the Bassani criterion. Similar results were confirmed for other metals. Examples of the aluminum shells computed are described in Fig. 9 using the three-dimensional computer graphics.

For the stage when deformation fully proceeded, a maximum thinning position was regarded as a fracture site in theory, and the initial fracture radius  $R_{cr}$  was compared theoretically and experimentally. The result is shown in Table 3, indicating again that the Bassani function predicts by far more actual values than Hill's function.

Figure 10 shows the comparison of yield loci on the quadrant I of the  $\sigma_\theta - \sigma_\phi$  plane between the Bassani and Hill functions. The Hosford yield locus is also added to the figure as a  $\sigma_1 - \sigma_2$  relation involving planar anisotropy, where  $\sigma_1$  is a principal stress in the rolling direction. The points A and B indicate the equibiaxial and plane-strain tensions in the Bassani locus, respectively. The corresponding stress points are denoted as C and D in the Hill locus and as E and F in the Hosford locus, respectively. From the figure, we

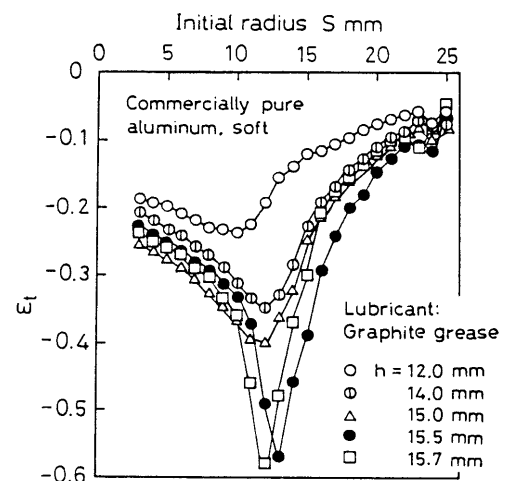
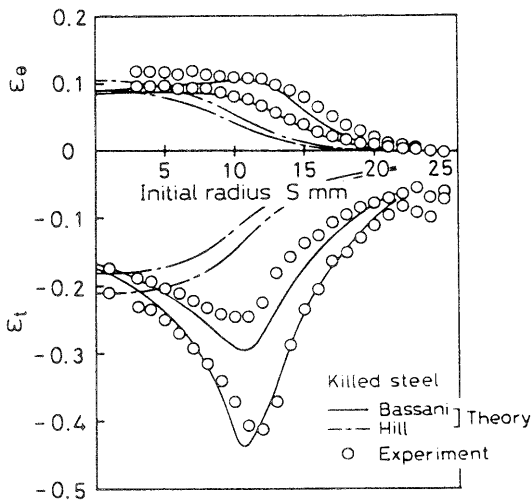


Fig. 7 Distribution of measured thickness strain

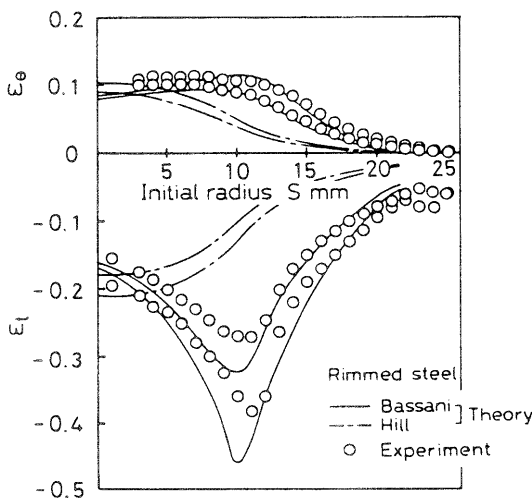
Table 3 Comparison of theoretical and experimental fracture radii

Materials	Theory		Experiment
	Hill	Bassani	
Killed steel	2	11	13.0
Rimmed steel	1	10	11.9
Commercially pure aluminum, soft	1	12	11.8
OFHC, soft	1	15	13.8

Unit : mm



(a)



(b)

Fig. 8 Comparison of theoretical and experimental strain distributions

see  $\sigma_{\theta A} > \sigma_{\theta C}$  and  $\sigma_{\theta B} / \sigma_{\theta A} > \sigma_{\theta D} / \sigma_{\theta C}$ , where the suffixes A~D are related to the aforementioned stress points. The former relation demonstrates that the Bassani criterion can express a so-called anomaly, while the latter means that the Bassani locus is rather near the Tresca locus. These yielding characteristics were confirmed for all the other metals used. The low  $\sigma_{\theta}$  value means that material strengthening is weak due to a change of stress path, and thus the strain is apt to concentrate locally. This is the reason why an intensive concentration of  $\epsilon_r$  occurs in the case of a Bassani function, as seen in Figs. 6 and 8. Concerning the Hosford locus, it can also express the anomaly, and its equi-biaxial point (E) is closer to the corresponding point in the Bassani locus (A) than in the Hill locus (C). Taking into account this result and the equivalence in yielding between the equi-biaxial and through-thickness simple compressive stresses<sup>(7)</sup>, it is deduced that, under a low friction condition causing a stress state close to simple compression, the Hosford yield function facilitates a more accurate estimation of  $\mu$  than Hill's.

Finally, the following can be said : The deforma-

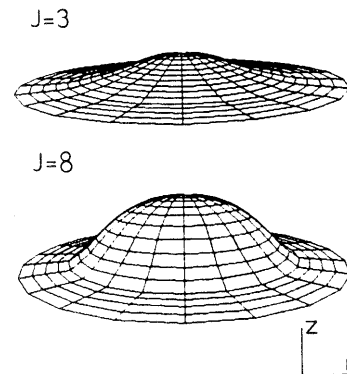


Fig. 9 Three-dimensional graphics of the aluminum shells calculated

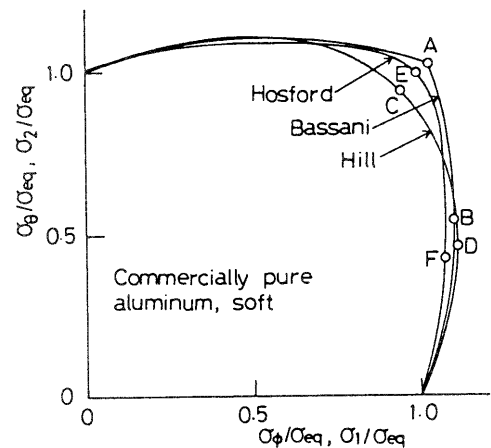


Fig. 10 Yield loci of aluminum sheets

tion of the sheets under biaxial tension is sensitive to a shape of yield locus, in other words, anisotropic yielding; the actual sheets possess more or less an anomaly; their yield stresses under plane-strain tension are relatively low; since the Bassani function can well express these characteristics, it is useful for the computer simulation of pure stretch-forming.

#### 4. Concluding Remarks

Based on the Bassani yield function, pure stretch-forming was numerically analyzed, and a simulation accuracy of strain distribution was examined. In addition, as a new test for estimating the friction coefficient, the strip compression method applicable to materials having planar anisotropy was proposed by extending Hill's method. It was thus concluded that the Bassani function affords a marked improvement with regard to the predictions of the strain distribution and the radial position of necking or fracture initiation, and thus such an unreasonable adjustment with the  $\mu$  values as done in past investigations becomes unnecessary. This result suggests that the deformation of metal sheets in pure stretch-forming is sensitive to a shape of the yield locus, and some yield function which can express exactly anisotropic properties including an anomaly should be employed to facilitate an accurate computer simulation. The Bassani function is regarded as a possible candidate, but from the limited nature of the present work, it is difficult to affirm that this criterion is best. Much closer observation and understanding of the shape of yield loci seem to be key points for solving the computer simulation problem.

#### References

- (1) Kaftanoglu, B. and Alexander, J. M., On Quasistatic Axisymmetrical Stretch Forming, *Int. J. Mech. Sci.*, Vol. 12, No. 12 (1970), p. 1065.
- (2) Plastic Working Research Group, *Jpn. Soc. Mech. Eng., Methods for Measuring Friction Coefficients in Plastic Working*, *J. Jpn. Soc. Tech. Plast.*, (in Japanese), Vol. 9, No. 87 (1968), p. 252.
- (3) Hill, R., A Theory of the Yielding and Plastic Flow of Anisotropic Metals, *Proc. R. Soc. L.*, Vol. 193, A (1948), p. 281.
- (4) Kurosaki, Y., Tokiwa, M. and Murai, K., Studies on Anisotropic Yield Characteristics and Press Formability of Metal Sheets (1st Rep., Estimation of Friction Coefficients in the Compression Test), *Proc. of Jpn. Soc. Tech. Plast. Spr. Conf.*, (in Japanese), (1984), p. 469.
- (5) Bassani, J. L., Yield Characterization of Metals with Transversely Isotropic Plastic Properties, *Int. J. Mech. Sci.*, Vol. 19, No. 11 (1977), p. 651.
- (6) Vial, C., Hosford, W. F. and Caddell, R. M., Yield Loci of Anisotropic Sheet Metals, *Int. J. Mech. Sci.*, Vol. 25, No. 12 (1983), p. 899.
- (7) Kurosaki, Y., Tokiwa, M. and Murai, K., Studies on Anisotropic Yield Criteria and Press Formability of Metal Sheets (Investigation into Bassani-Type Criteria), *Bull. JSME*, Vol. 29, No. 255 (1986), p. 3202.
- (8) Kurosaki, Y. and Matsumoto, M., Deformation and Formability in Bore-Expanding of Metal Sheets from the Aspect of Anisotropic Yield Characteristics, *Advanced Technology of Plasticity*, Vol. 2 (1987), p. 689, Springer-Verlag.
- (9) Woo, D. M., Analysis of the Cup-Drawing Process, *J. Mech. Eng. Sci.*, Vol. 2, No. 2 (1964), p. 116.
- (10) Kobayashi, M., Kurosaki, Y. and Kawai, N., Influences of Friction and Metal Properties on Pure Stretchability of Sheet Metals, *Trans. ASME*, Vol. 102, No. 2, B (1980), p. 142.
- (11) Woodthorpe, J. and Pearce, R., The Anomalous Behaviour of Aluminium Sheet under Balanced Biaxial Tension, *Int. J. Mech. Sci.*, Vol. 12, No. 4 (1970), p. 341.